Effects of Heating Media on Microstructure and Chemical Composition of Heat-treated *Pometia pinnata*

Caishan Ling,[a] Chenyang Cai,[a,b,*] Xianqing Xiong,[a,b,*] and Yunfang Shen [c]

Changes of microstructure, crystallization, chemical composition, and equilibrium moisture content (EMC) of heat-treated wood (HTW) were investigated to explore the effects of heating media (saturated steam, superheated steam, air) and heat treatment (HT) temperature on HTWs. The results showed that the saturated steam induced more severe cell wall destruction than the other two media. Although the porosity slightly increased with the increasing HT temperature, superheated steam and air HT still decreased the porosity compared to that of control, whereas saturated steam HT increased the porosity. The HT increased both relative crystallinity and crystal size of HTWs. The increasing HT temperature slightly increased the relative crystallinity but decreased the crystal size. The highest crystallinity (55.0%) was observed after saturated steam HT. Leaching led to the increase of crystal size of HTW treated in saturated steam (about 0.15 nm), while those treated in unsaturated steam and air decreased. The increase in relative amount of lignin and cellulose due to the hemicellulose degradation were the main chemical changes of HTWs. Further lignin condensation reaction only occurred after saturated steam HT. Although saturated steam HT induced increased porosity, its lowest EMC (5.91%) indicated the decrease of hydroxyl groups.

DOI: 10.15376/biores.19.4.7320-7338

Keywords: Heating media; Heat treatment; Microstructure; Crystallinity; FTIR; XRD; SEM

Contact information: a: Department of Furniture Design, College of Furnishings and Industrial Design, Nanjing Forestry University, Nanjing 210037, China; b: Co-Innovation Center of Efficient Processing and Utilization of Forest Resources, Nanjing Forestry University, Nanjing 210037, China; c: Zhejiang Shenghua Yunfeng Greeneo Co., Ltd., Huzhou 313299, China;
** Corresponding authors: chenyangc@hotmail.com; xiongxianqing@njfu.edu.cn*

INTRODUCTION

Heat treatment (HT) is an effective and commercial technology for improving the physical and chemical properties of wood and its products (Pelit *et al.* 2016; Hill *et al*. 2021). Commercial HT processes usually take place at temperatures between 160 and 240 °C with different heating media, for example, superheated steam, nitrogen, hot oil, vacuum, *etc*. (Gérardin 2016). Usually, heat treatment with temperatures between 60 and 200 °C is called mild HT (Obataya and Tomita 2002). Mild HT can improve the dimensional stability of wood without significant loss of mechanical strength and reduce the color change caused by carbonization (Cao *et al*. 2022).

The HT results in weight loss (Czajkowski *et al*. 2020), changes in mechanical strength, and reduction in equilibrium moisture content (EMC) and hygroscopicity, which subsequently improves the dimensional stability (Borůvka *et al*. 2019) and decay resistance (Cao *et al*. 2011). These property changes mainly result from the degradation of chemical constituents (hemicellulose, cellulose, and lignin) (Wang *et al*. 2018) and changes of pore

structure (Sun *et al*. 2022). During the HT process, the decrease of -OH groups (Xu *et al*. 2022) due to the degradation of hydrophilic hemicellulose, and the increase of relative crystallinity (Andersson *et al*. 2005) due to the breakdown and loss of some hemicellulose, would decrease the hygroscopicity of heat-treated wood (HTW). In addition, the shrinkage and degradation of the wood cell wall at elevated temperature affects the integrity and distribution of pores, which also makes an impact on the sorption property of HTW (Zauer *et al*. 2013; Cai *et al*. 2020). The decrease in the porosity of the HTW would also cause the decrease of hygroscopicity (Hill *et al*. 2006; He *et al*. 2023). Thus, the moisture content and the water absorption of HTW are reduced significantly.

Some research claims that the changes in properties of HTW are also affected by the moisture conditions (depending on the heating media) applied in HT process (Endo *et al*. 2016; Hill *et al*. 2021). HT under a wet condition results in greater mass loss compared with HT under dry condition, especially when a post-treatment water-leaching is performed (Pockrandt *et al*. 2018). The presence of water accelerates hydrolysis process, and the acetic acid generated from hemicellulose degradation further promotes the degradation of polysaccharides into water soluble degradation products, which could be removed by leaching (Čermák *et al*. 2016; Marcon *et al*. 2021). At the same treatment temperature, the hygroscopicity of HTWs treated in wet condition reduces greater than those treated in moist and dry conditions because of the higher amount of moisture in heating medium that promotes the degradation of hydrophilic hemicellulose (Liu *et al*. 2023). The HTWs processed in wet and dry conditions also show different behaviors after moistening. Some scholars observed that the volume of HTW manufactured by wet HT process was reversible after undergoing dry-wet cycles, while no similar reversible change was observed in the HTW made under dry conditions (Altgen *et al*. 2016; Obataya *et al*. 2017). The HTW produced in wet condition showed lower dimensional stability than that in dry condition. In contrast, Hill *et al*. (2021) concluded that the reduced EMC due to dry HT was partially reversible, but it did not occur in HTW produced in wet condition. The explanation was that the stress remained in amorphous region when wood was heated in dry condition, while the high moisture level helped the stress relaxation during HT in wet condition. Furthermore, Endo *et al*. (2016) found that the hygroscopicity reversibility was clearer after HT at 60% heating relative humidity (HRH) than HT at 0% HRH, while HTWs heated at 92% HRH or above had no reversibility, indicating that the HT in dry and moist condition might cause temporary effect on hygroscopicity reduction. Simultaneously, the crystallization state of cellulose was also affected by the moisture content of HT. The crystallinity of HTW treated under dry conditions significantly decreases after the dry-wet cycle, while the wood treated under wet conditions does not show substantial changes (Sun *et al*. 2022).

The hygroscopicity of wood is affected by the changes of the chemical composition and microstructure of cell walls. Despite the comprehensive literature on the hygroscopicity of HTW (Hill 2006), there is limited comparison and information concerning the anatomic and chemical changes in HTW treated with different heating media (Sun *et al*. 2022), given that most studies focus on the influence of temperature and time on wood.

Pometia pinnata is a material widely distributed in southeastern Asia. It has beautiful grain and relatively high hardness and is mainly utilized in the fields of furniture manufacturing and flooring. However, during its usage as flooring for ground with heating system, it would be subjected to a more severe environment compared to normal flooring. In this case, investigating the changes of water-related properties caused by mild heat

treatments to improve the dimensional stability and keep the original color of *Pometia pinnata* wood is necessary. In this study, *Pometia pinnata* wood was heat treated in three different media (*e.g.*, saturated steam, superheated steam, and air) with a duration of 2 h. The anatomic structure, relative crystallinity, chemical composition, and EMC of HTW treated in three different moisture conditions were analyzed and compared. The results of this study would be beneficial for understanding the mechanism of changes in HTW properties under different heating media and providing guidance for the optimization of processing technology of HTW.

EXPERIMENTAL

Materials

Pometia pinnata sawn timbers with a dimension of approximately 930 mm (length) × 130 mm (width) × 19 mm (thickness) provided by Zhejiang Shenghua Yunfeng Greeneo Co. Ltd were used as study materials. All timbers were first kiln dried at 60 °C for 8 weeks, and then conditioned at room temperature until the moisture content of wood reached 11% ± 0.5% before HT.

Heat Treatment

Timbers were further sawn into 450 mm (length) × 60 mm (width) × 19 mm (thickness), and then heat treated with different parameters. The treatment details are shown in Table 1. Samples were treated at 140 and 160 °C, respectively, for 2 h. Saturated steam, superheated steam, and air were used as media for different treatment groups. For water-leaching process, samples were soaked into warm water (60 °C) for 1 h immediately after HT. Afterwards, the wet samples were mildly dried at 50 °C for two weeks and conditioned at 20 °C 65% RH until their moisture content became constant and the EMC achieved. Untreated boards, originating from the same materials as the heat-treated ones, were used as controls. Fifteen replicates were prepared for each group (Table 1).

Table 1. Heat Treatment Parameters of Samples

Group	Code	Medium	Temperature (°C)	Leaching or Not
1	Control	\	\	\
2	Sat4-0	Saturated Steam	140	No
3	Sat4-1		160	Yes
4	Sat6-0		140	No
5	Sat6-1		160	Yes
6	Sup4-0	Superheated Steam	140	No
7	Sup4-1		160	Yes
8	Sup6-0		140	No
9	Sup6-1		160	Yes
10	Air4-0	Air	140	No
11	Air4-1		160	Yes
12	Air6-0		140	No
13	Air6-1		160	Yes

Anatomic Structure Analysis

Scanning electron microscopy (SEM)

Wood slices of 10 mm (radial) × 10 mm (tangential) × 2 mm (longitudinal) were prepared from each sample was used as specimen for SEM test. The cross-section of the specimens was smoothed by sliding microtome to obtain an even surface for observations. Then, the anatomic morphology of specimens with different treatments were captured using SEM (Quanta 200, FEI, Hillsboro, OR, USA).

Nitrogen adsorption analysis

Powder with ø = 0.25 mm was milled from specimens of each HT group, and oven-dried before nitrogen gas adsorption experiment. The pore structure was analyzed by a specific surface area/porosity analyzer (ASAP2460, Micromeritics, Norcross, GA, USA) at 77.4 K. The specific surface area (SBET) was calculated according to Brunauer-Emmett-Teller (BET) methods (Brunauer *et al*. 1938) and the pore size distribution was determined according to Barrett-Joyner-Halenda (BJH) methods (Barrett *et al*. 1951).

X-ray Diffraction (XRD) Analysis

Specimens were milled into fine powder with diameter of 0.15 mm for the XRD analysis. The crystalline structures of heat treated, and control specimens were analyzed using a XRD (Ultima IV, Rigaku Ltd., Tokyo, Japan) spectrometer with Cu Kα radiation from 2θ = 5° to 45°, and the scanning speed was 5° min^{-1}.

The crystallinity index (CrI) of specimens were calculated according to Segal method (Thygesen *et al*. 2005), Eq. 1,

$$CrI(\%) = \frac{I_{002} - I_{am}}{I_{002}} \times 100 \quad (1)$$

where I_{002} was the intensity of the crystalline peak at 2θ =22° to 23°, and I_{am} was the minimum intensity at 2θ =18° to 19°.

The width of the crystal obtained from (200) diffraction was obtained based on Scherrer method (Newman 1999), as shown in Eq. 2,

$$D = \frac{k\lambda}{B\cos\theta} \quad (2)$$

where D was the width of crystal, k was the Scherrer constant (0.9), λ was the wavelength of the X-rays, B was the half-bandwidth in radians, and θ was the Bragg angle.

Fourier Transform Infrared (FTIR) Spectroscopy

The FTIR spectrum of each specimen was recorded with FTIR spectrometer (VERTEX 80V, Bruker, Germany) in the range of 4000 to 400 cm^{-1} with a resolution of 4 cm^{-1}. Each spectrum was collected from 32 scans in the absorbance mode. Specimens for FTIR analysis were dried, milled, and mixed with KBr in a ratio of about 1:25, and compressed under vacuum to form pellets. The spectra were normalized to the band at 2902 cm^{-1} (Peng *et al*. 2022).

EMC measurement

The specimens with dimensions of 20 mm (radial) × 20 mm (tangential) × 20 mm (longitudinal) were first oven-dried at 105 °C until constant mass, and then they were conditioned at 20 °C 65% RH for about 1 month until the weight remained. The EMC was calculated based on the oven-dry mass and the mass after conditioning.

RESULTS AND DISCUSSION

SEM Analysis

Changes in cell wall structure due to different HT parameters are shown in Fig. 1. Figure 1 demonstrates that without water-leaching process, the treatment temperature of 140 °C did not affect the microstructure of specimen regardless of the heating media. After the specimens were subjected to leaching process, a few cracks were observed in the cell wall of specimens treated in saturated steam and in superheated steam, while the specimens treated in air condition did not show obvious difference in cell wall structure compared with that of controls. At the treatment temperature of 160 °C, collapse of cells and more cracks in cell wall were observed in the saturated steam treated specimens. Superheated steam HT and air HT at 160 °C also led to a damaged microstructure, for example, more holes near the compound middle lamella were found in those HTW groups. The further water leaching process emphasized the holes and cracks caused by HT and led to a greater extent of cell wall degradation. Such degradation resulted in the collapse in cell wall, merging in cell lumens and a more brittle morphological structure.

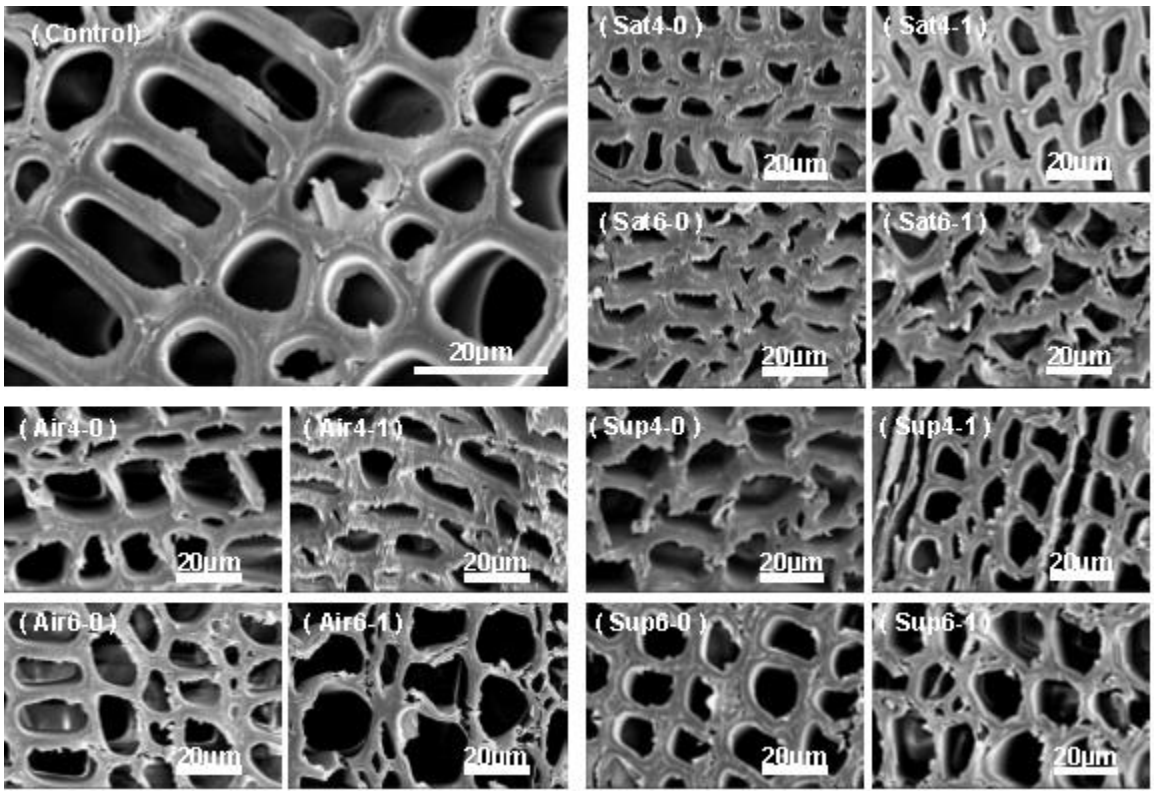

Fig. 1. SEM images of control and HTWs (Sat: Saturated steam, Sup: Superheated steam, Air: Air; 4: 140 °C, 6: 160 °C; 0: Without leaching, 1: Leaching)

The holes and cracks in cell wall generated during HT were mainly caused by the degradation of chemical components, mainly hemicellulose (Elisabeth and Gerd 2008; Wang and Howard 2018)) and the anisotropic shrinkage of different cell wall layers (Biziks *et al*. 2013; Wu *et al*. 2021). The structural destruction degree would be affected by the heating media. The higher treatment temperature (Jang and Kang 2019) and the presence of moisture (Ali *et al*. 2021; Obataya *et al*. 2021) in saturated steam and superheated steam

would promote the hydrolysis of cell wall components, making the cell wall more degraded and less intact compared with that treated in air condition. Saturated steam led to greater degradation, followed by superheated steam. During the leaching post-treatment, the water removed the degradation products and interacted with the acids formed during HT, which facilitated the cell wall destruction (Lê *et al*. 2016; Hill *et al*. 2021). The changes in microstructure would also affect the pore structure of HTW (Obataya *et al*. 2017).

Nitrogen Adsorption Analysis

The nitrogen adsorption method was applied to study the change of pore structure after various HT. Quasi-equilibration might be induced during the nitrogen adsorption, which would cause underestimation of micropores (Shi and Avramidis 2018; Broda *et al*. 2019). However, the results obtained by this method still can be used for making a comparison between HT groups. As illustrated in Fig. 2, the nitrogen adsorption-desorption isotherms of all specimens were similar in shape, with complete and smooth curves, and consistent change trends. According to the classification of International Union of Pure and Applied Chemistry (IUPAC), the isotherms of both treated and control specimens were of type II, with a H3-type hysteresis loop.

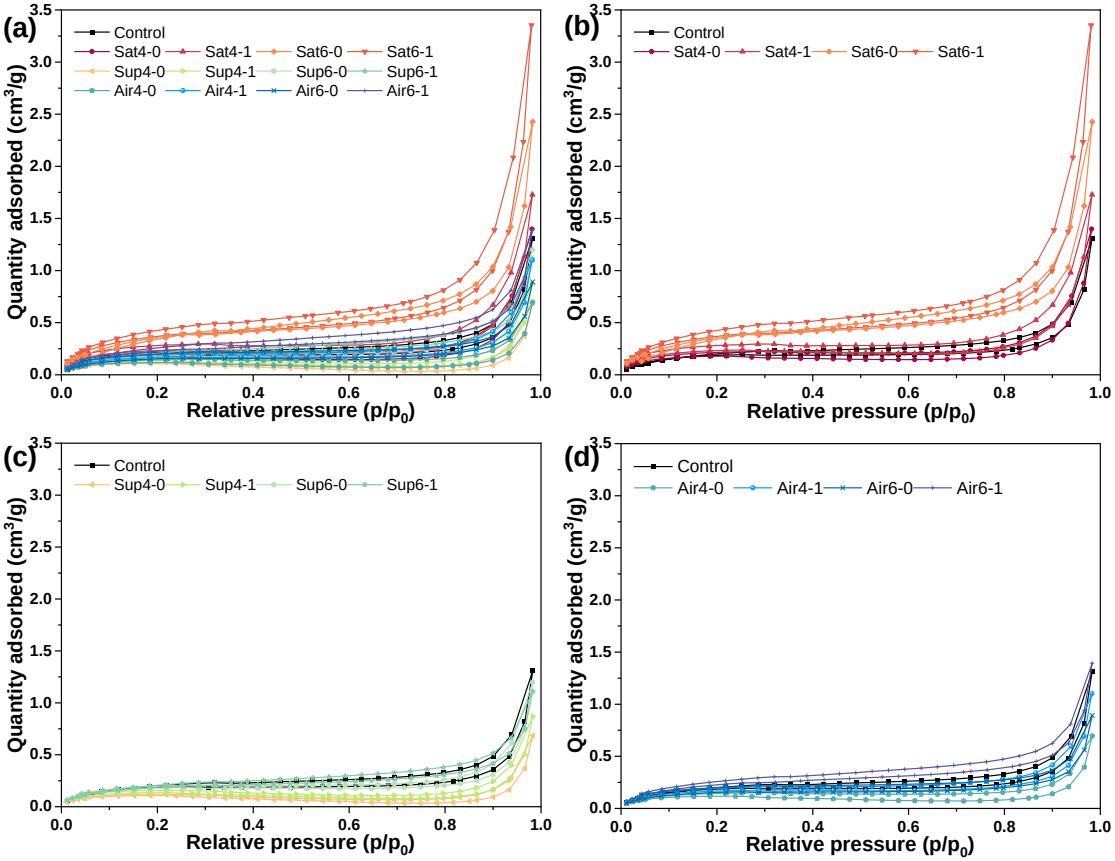

Fig. 2. Nitrogen adsorption-desorption isotherms (a: isotherms of all groups; b, c, d: isotherms of saturated steam groups, superheated steam groups and air groups, respectively)

This result indicated the existence of slit-shape pores in all HTWs and control, which coincided with the previous research by Yin *et al*. (2015). The HT with saturated steam at 160 °C, both with and without water leaching treatments, increased the adsorption

amount obviously, while HT with superheated steam and air at 140 ℃ showed a clear reduction. The curves of the rest of the HT groups overlapped partly with the control.

The total pore volume and average mesopore diameter were estimated based on the cylindrical pore model using the BJH method (Barrett *et al*. 1951). The parameters describing N_2 adsorption capacity, the surface area (S_{BET}), N_2 volume between 1.7 to 300 nm (V_{total}), and average diameter (D_{BJH}) of the mesopores are listed in Table 2. The results showed that the higher the N_2 adsorption capacity, the bigger the S_{BET} and V_{total}. Compared to the control, the nitrogen adsorption capacity, S_{BET}, and V_{total} of the saturated steam treated HTW increased, while that of the superheated steam and air treated wood mainly decreased. This was partly inconsistent with the results reported by Liu *et al*. (2023), who reported that the S_{BET} and V_{total} were both decreased no matter in saturated steam or in air condition at 180 and 210 °C. However, Sun *et al*. (2022) found that the porosity of heat-treated larch first increased and then decreased with the increasing treatment temperature, indicating the change of porosity was related with the intensity of HT. Higher HT temperature and leaching post-treatment mostly induced an increase in porosity; however, the higher HT temperature also resulted in a decrease in the average mesopore diameter.

Table 2. The N_2 Adsorption Capacity, Surface Area, Total Pore Volume, and Average Pore Diameter of Specimens

Group	Code	Max Adsorption Capacity of N_2 ($cm^3 \cdot g^{-1}$)	S_{BET} ($m^2 \cdot g^{-1}$)	V_{total} ($mm^3 \cdot g^{-1}$)	D_{BJH} (nm)
1	Control	1.312	0.673	1.911	18.867
2	Sat4-0	1.398	0.557	2.010	20.270
3	Sat4-1	1.729	0.803	2.503	17.448
4	Sat6-0	2.428	1.294	3.688	15.407
5	Sat6-1	3.353	1.307	5.068	16.871
6	Sup4-0	0.685	0.319	0.947	23.286
7	Sup4-1	0.870	0.414	1.214	21.879
8	Sup6-0	1.198	0.586	1.722	18.087
9	Sup6-1	1.111	0.675	1.641	12.265
10	Air4-0	0.696	0.350	0.960	16.159
11	Air4-1	1.100	0.551	1.585	16.482
12	Air6-0	0.892	0.518	1.279	12.687
13	Air6-1	1.393	0.836	2.099	13.502

Because the number of pores cannot be directly related to the pore volume due to the various morphology and depth of different pores, the pore size distribution of all specimens represented by the pore volume in different ranges are shown in Table 3. The HT in saturated steam at 140 °C decreased the volume of micropores but increased the volume of meso- and macro-pores, whereas HT in saturated steam at 160 °C generally increased the volume of pores in all scales. In contrast, HT in superheated steam and air conditions normally resulted in a reduction of all kinds of pores.

Table 3. Pore Size Distribution of Both Control and HTWs (mm^3/g)

Group	Code	1.7 to 2 nm	2 to 50 nm	> 50 nm
1	Control	0.069	1.015	0.827
2	Sat4-0	0.021	1.132	0.856
3	Sat4-1	0.056	1.463	0.984
4	Sat6-0	0.116	2.192	1.380
5	Sat6-1	0.137	3.011	1.920
6	Sup4-0	0.008	0.451	0.488
7	Sup4-1	0.022	0.603	0.589
8	Sup6-0	0.055	0.908	0.759
9	Sup6-1	0.082	0.952	0.607
10	Air4-0	0.020	0.461	0.479
11	Air4-1	0.067	0.832	0.686
12	Air6-0	0.061	0.661	0.557
13	Air6-1	0.096	1.226	0.777

The changes in pore structure of HTW was an overall outcome of degradation and removal of wood components, as well as the changes of the microstructure. The shrinkage of cell wall, closer binding between the microfibers (Hill 2006), increase in crystallinity, and filling in the intermicellar pores by softening and flowing of lignin during HT (Cai *et al*. 2020) were probably the main reasons of the reduced porosity in the superheated steam and air HT groups. However, the further degradation and volatilization of cell wall chemical composition facilitated by the moisture in heating medium, especially the saturated steam (Jang and Kang 2019; Rahimi *et al*. 2019), would be the dominant reason for the increased micro- and mesopores in saturated steam HTWs. In contrast, the increase in the macropores could also be due to the collapse of cell wall and merging in cell lumens as shown in Fig. 1.

The removal of the degradation products by water leaching post-treatment explained its increased HTW's porosity (Kymäläinen *et al*. 2018; Willems *et al*. 2020). The intense HT temperature resulted in a decrease in the average mesopore diameter, which probably indicated the generation of smaller pores or increased proportion of smaller pores due to the physical and chemical degradation of wood occurred during HT (Junghans *et al*. 2005).

Crystallinity Analysis

The X-ray diffraction patterns, and the crystallization performance of all specimens are shown in Fig. 3 and Table 4. The higher crystallization not only contributes to the higher rigidity, but also reduces the hygroscopicity of wood. Within the scanning interval of 0 to 40°, two prominent refection peaks appeared on the curve. The one located at about 2θ = 18° denoted the scattering intensity of the diffraction angle in the amorphous area, whereas the other one appeared around 2θ = 22° and represented the maximum strength (I_{002}) of the diffraction angle in the crystalline area. The almost unchanged location and numbers of refection peak of all groups indicated that all HT methods did not transform the crystalline type of wood (Bhuiyan *et al*. 2000).

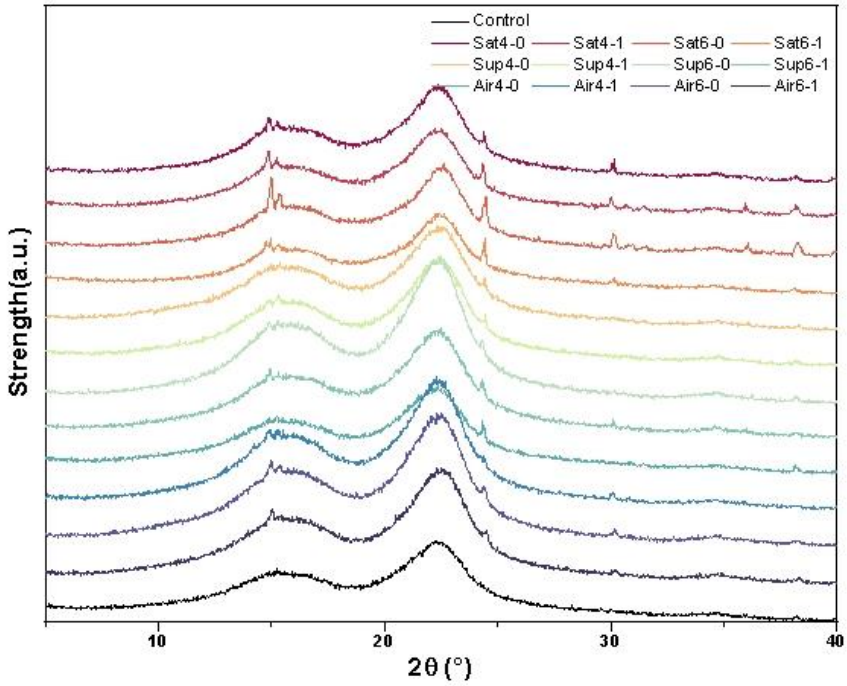

Fig. 3. Diffractograms of control and HTWs (Sat: Saturated steam, Sup: Superheated steam, Air: Air; 4: 140 °C, 6: 160 °C; 0: Without leaching, 1: Leaching)

Table 4. Crystallization Properties of Control and HTWs

Group	Code	Relative Degree of Crystallinity (%)	Crystal Size (nm)
1	Control	46.69%	0.23
2	Sat4-0	54.99%	0.36
3	Sat4-1	53.41%	0.51
4	Sat6-0	54.52%	0.25
5	Sat6-1	54.03%	0.42
6	Sup4-0	53.56%	0.33
7	Sup4-1	53.45%	0.23
8	Sup6-0	54.48%	0.31
9	Sup6-1	52.75%	0.24
10	Air4-0	49.03%	0.30
11	Air4-1	51.24%	0.18
12	Air6-0	54.64%	0.24
13	Air6-1	53.89%	0.23

According to Table 4, all HT methods increased the relative crystallinity of HTW, regardless of different heating media, which was attributed to the degradation of amorphous carbohydrates (Kim *et al*. 2010) and the rearrangement and reorientation of the cellulose and hemicellulose molecular chains (Olek and Bonarski 2014). Among three media, saturated steam had the greatest improvement of relative crystallinity, followed by superheated steam and air, respectively. This result was consistent with Bhuiyan *et al*.

(2000), who found that the high humidity in HT conditions would promote the crystallization in both pure and wood cellulose. The relative crystallinity of HTWs was slightly increased by increasing the treatment temperature from 140 to 160 °C. This was also consistent with the previous studies (Zheng *et al*. 2016; Durmaz *et al*. 2019), and the reason for the increased relative crystallinity was the degradation of hemicellulose and the amorphous cellulose at elevated temperature (Birinci *et al*. 2022; Wang *et al*. 2022). The result showed the water leaching post-treatment only led to negligible decrease in relative crystallinity. However, Altgen and Militz (2016) claimed that water-leaching can restore the mobility of the structure and rearrange the molecular chains within the cell wall, which could promote the increase of relative crystallinity.

The crystal size also reflects the crystallization performance of wood. As shown in Table 4, all HT methods, except Air4-1, increased the crystal size of wood to a certain extent. Among all media, saturated steam had the highest increase in crystal size, followed by superheated steam and air, indicating that high moisture condition promoted crystallization (Hill *et al*. 2021). Regardless of heating media, although the relative crystallinity slightly increased with the increasing HT temperature, the crystal size of HTWs decreased. This result was partly inconsistent with Dwianto *et al*. (1996), who found the crystal size was increased in air HT condition, while it was decreased in saturated steam condition with the increasing treatment temperature. However, other researchers (Andersson *et al*. 2005; Cheng *et al*. 2017) discovered that the crystal size would firstly increase and then decrease, and then increase again with the rising temperature. Water leaching resulted in a decrease in crystal size of HTWs treated in superheated steam and air conditions. However, it was surprising to find the crystal size of saturated steam HTWs increased after leaching. There was no convincing reason to explain the increase in saturated steam HTW after leaching; however, the reorganization of cellulose molecules during water leaching and further oven-dry process before XRD analysis might partly explain this phenomenon (Altgen and Militz 2016). The increase of relative crystallinity and grain size would reduce the hygroscopicity and increase the strength of cell wall (Wang *et al*. 2024), which meant that, in this research, the wood leached after treated in saturated steam at 160 °C could gain the highest dimensional stability and cell wall strength.

Chemical Composition Analysis

The characteristic FTIR spectra of wood with different HT methods are shown in Fig. 4. The assignment of signals is shown in Table 5.

The peaks at 1739 cm^{-1} refer to the vibration of carboxylic groups (C = O) of the non-conjugated acetyl group in hemicelluloses. Compared to control, the saturated steam treated specimens showed a clearer decrease in the intensity of peak than that of superheated steam and air treated groups, indicating severer breakage of acetyl side chain and degradation of hemicelluloses during saturated steam HT (Guo *et al*. 2015; Li *et al*. 2015). Such a decrease was more evident with the increasing HT temperature. Degradation of hydrophilic hemicellulose could reduce the hygroscopicity of HTW. The acetic acid produced by the degradation of hemicellulose would further promote the depolymerization of amorphous polysaccharides and catalyze the degradation and condensation reactions of lignin, which will lead to a decrease in the number of carbon matrices (Hill *et al*. 2021).

The peak at 1625 cm^{-1} corresponded to the H-O-H deformation vibration of absorbed water. The decrease at this band after all HT groups might be attributed to the decreased water accessibility caused by the dehydration and deacetylation reaction during HT process (Bryne *et al*. 2010).

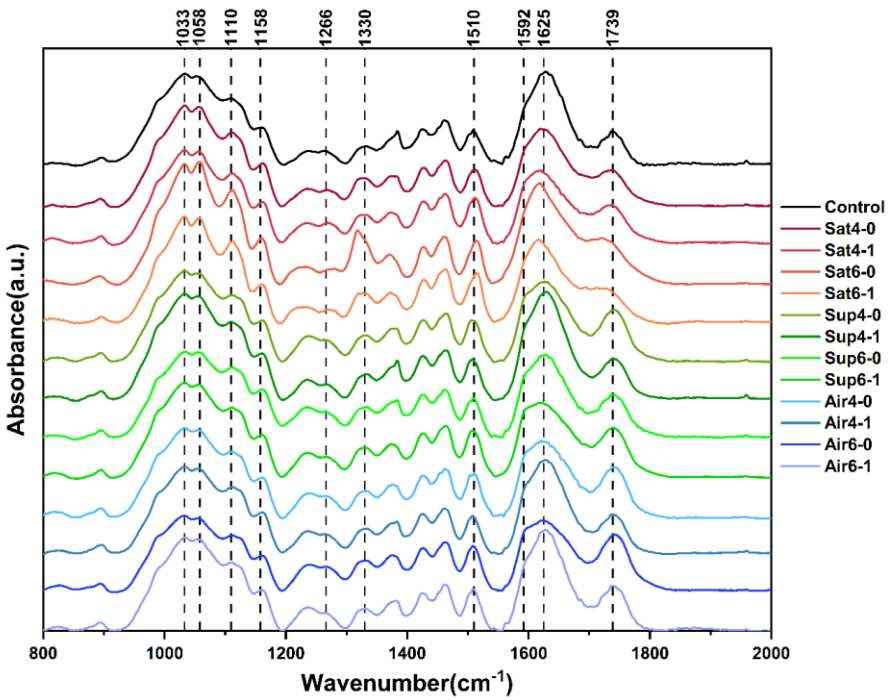

Fig. 4. FTIR spectra of control and HTWs (Sat: Saturated steam, Sup: Superheated steam, Air: Air; 4: 140 °C, 6: 160 °C; 0: Without leaching, 1: Leaching)

Table 5. Assignment of the FTIR Signals for Wood Constituents

Wavenumber (cm^{-1})	Assignments	References
1739	-C=O of non-conjugated aldehyde	Kotilainen *et al*. (2000); Özgenç *et al*. (2017)
1625	Absorbed water	Marcon *et al*. (2021)
1592	Aromatic skeletal vibrations and the -C=O stretch in lignin	Zylka *et al*. (2009); Hillis and Rozsa (1978)
1510	-C=C- stretching of the aromatic skeletal vibrations (lignin)	Colom *et al*. (2003); Temiz *et al*. (2007)
1330	-OH in plane bending (cellulose)	Kotilainen *et al*. (2000)
1266	Guaiacyl-ring (lignin)	Kotilainen *et al*. (2000)
1158	-C-O-C symmetric stretching (cellulose)	Kotilainen *et al*. (2000); Özgenç *et al*. (2017)
1110	-C=C stretching (cellulose)	Kotilainen *et al*. (2000); Nuopponen (2005)
1058	-C-O stretching (cellulose)	Özgenç *et al*. (2017)
1033	-C-O and -C=O stretching in cellulose, symmetric -C-O-C stretching of dialkyl ethers, aromatic -C-H deformation in lignin	Hakkou *et al*. (2005); Nuopponen (2005)

An increase at this band was observed after water leaching post-treatment in superheated steam and air HT groups, indicating the increase of water affinity after leaching (Endo *et al*. 2016; Marcon *et al*. 2021). However, it was surprising to find that saturated steam HT showed a remarkable reduction at this band after leaching, implying decrease of water affinity of saturated steam treated wood after leaching.

The lignin peaks at 1592, 1510, and 1266 cm^{-1} increased in all HT groups, and the intensity of these peaks increased slightly with the increasing HT temperature. This result might be due to the increase of the relative amount of lignin due to the degradation of polysaccharides during HT (Kučerová *et al*. 2019). In addition, the peak at 1510 cm^{-1} shift to 1514 cm^{-1} after HT at 160 °C in saturated steam condition, suggesting the condensation reaction caused by the cleavage of the aliphatic side chain and the cleavage of the β-O-4 connection in the lignin structure (Sikora *et al*. 2018; Jang and Kang 2019). However, this kind of change was not observed in the other two media, indicating the superheated steam HT and air HT did not affect lignin at mild temperature, while the saturated steam HT could cause lignin reaction at the same treatment temperature. Ding *et al*. (2011) reported the high-pressure applied during saturated steam HT could facilitate the degradation of wood. Different changes of the peak at 1510 cm^{-1} were reported previously. For example, Li *et al*. (2015) found such peak intensity in heat-treated teak wood with steam increased slightly with increasing temperature. Özgenç *et al*. (2017) found the intensity of this peak of air HT pine and spruce decreased, while that of beech increased. Moreover, Windeisen *et al*. (2007) found this peak increased in softwood but remained unchanged in hardwood. The reason for the differences between the above-mentioned studies might be due to the different tree species and HT methods. The condensation reaction in the lignin structure might cause the decrease of hygroscopicity.

The increased intensity at 1330 cm^{-1} was detected in all HT groups, particularly in saturated steam groups. This signal was primarily assigned to the cellulose and was related to the content of crystallized cellulose I (Colom *et al*. 2003), indicating the increase in crystallinity after HT. This change was consistent with the results of the relative crystallinity obtained by X-ray diffraction. In addition, the changes in the HTWs at 1033, 1058, 1158, and 1110 cm^{-1} were mainly related to cellulose and, to a lesser extent, lignin. The increase in the intensity of these peaks indicated the increased concentrations of the alcohol and/or carboxyl groups in cellulose (Bhuiyan and Hirai 2005).

EMC Analysis

Figure 5 shows the EMC of the specimens determined after conditioned at 20 °C 65% RH. The results showed that HT significantly reduced the EMC of all specimens. The decrease of the wood EMC depended on the heating medium and HT temperature. The saturated steam HT reduced the EMC to a greater extent than the superheated steam HT and air HT. No significant difference was observed between the latter two heating media. According to the pore structure and FTIR results obtained in this study, compared to superheated steam HT and air HT, saturated steam HT tended to promote hemicellulose degradation and lignin condensation, and to improve the crystallinity, but also it increased the porosity. The lowest EMC achieved in saturated steam group indicated the changes in wood components was the predominate reason for the decreased hygroscopicity than the changes of cell wall pore structure. Higher HT temperature resulted in lower EMC because of the elimination of hemicellulose hydroxyl groups (Phuong *et al*. 2007) and increase of the crystallinity by elevated temperature (Zhao *et al*. 2023), which corresponds with previous research (Bayani *et al*. 2019; Cai *et al*. 2020).

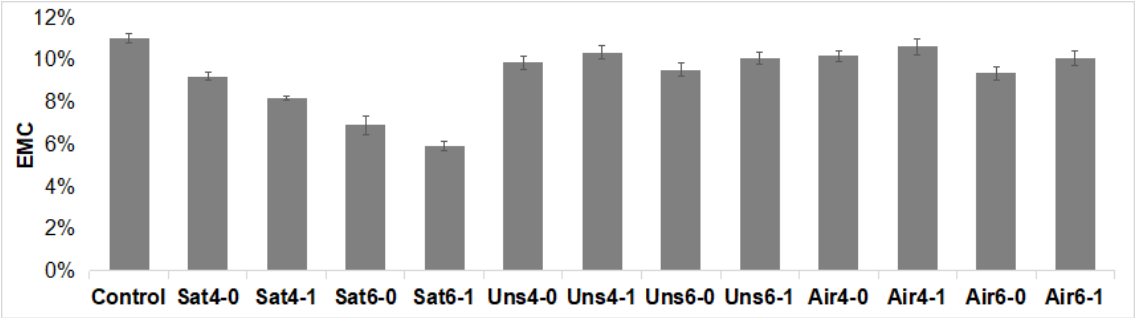

Fig. 5. The EMC of control and HTWs

Surprisingly, the water leaching post-treatment did not affect the EMC of different groups in a consistent way. Leaching decreased the EMC of superheated steam HTWs, whereas it increased the EMC of superheated and air HTWs. However, this finding was also in accordance with the above XRD and FTIR results, which showed leaching increased the crystal size and decreased the absorbed water band of the saturated steam treated specimens.

CONCLUSIONS

1. The heat treatment (HT) induced cracks and holes in the cell wall. Such destruction was more prone to occur after saturated steam HT than superheated steam or air HT. Porosity of cell wall decreased after superheated steam HT and air HT, whereas it increased after saturated steam HT.
2. Compared to the other two heating media, saturated steam induced the greater degradation of hydroxyl groups, and the lignin condensation reaction was only observed after saturated steam HT at 160 °C. This indicates that using saturated steam as a heat treatment medium can achieve a higher degree of dimensional stability improvement in wood at relatively lower temperatures.
3. The water leaching post-treatment tended to an increase in the porosity, decreased the relative crystallinity, and subsequently increased the EMC of HTWs by superheated steam and air HT. In contrast, the crystal size of saturated steam treated wood increased after leaching.
4. The best treatment in this study was treating wood in saturated steam at 140 °C and leaching after heat treated for 2 hours. In the mild temperature heat-treatment stage, saturated steam was more helpful to reduce the hygroscopicity of wood than unsaturated steam and air. Therefore, saturated steam could be used to reduce the hygroscopicity during mild temperature heat-treatment. In future research, the influence of heat treatment medium on wood color, mechanical properties and other properties could be studied.

ACKNOWLEDGMENTS

The authors are grateful for the support of the National Natural Science Foundation of China, Grant No. 32301521.

REFERENCES CITED

Ali, M. R., Abdullah, U. H., Ashaari, Z., Hamid, N. H., and Hua, L. S. (2021). "Hydrothermal modification of wood: A review," *Polymers* 13(16), article 2612. DOI: 10.3390/polym13162612

Altgen, M., Hofmann, T., and Militz, H. (2016). "Wood moisture content during the thermal modification process affects the improvement in hygroscopicity of Scots pine sapwood," *Wood Sci. Technol.* 50, 1181-1195. DOI: 10.1007/s00226-016-0845-x

Altgen, M., and Militz, H. (2016). "Influence of process conditions on hygroscopicity and mechanical properties of European beech thermally modified in a high-pressure reactor system," *Holzforschung* 70(10), 971-979. DOI: 10.1515/hf-2015-0235

Andersson, S., Serimaa, R., and Väänänen, T. (2005). "X-ray scattering studies of thermally modified Scots pine (*Pinus sylvestris* L.)," *Holzforschung* 59(4), 422-427. DOI: 10.1515/HF.2005.069

Barrett, E. P., Joyner, L. G., and Halenda, P. P. (1951). "The determination of pore volume and area distributions in porous substances. I. Computations from nitrogen isotherms," *J. Am. Chem. Soc.* 73(1), 373-380. DOI: 10.1021/ja01145a126

Bayani, S., Taghiyari, H. R., and Papadopoulos, A. N. (2019). "Physical and mechanical properties of thermally-modified beech wood impregnated with silver nano-suspension and their relationship with the crystallinity of cellulose," *Polymers* 11(1), article 1538. DOI:10.3390/polym11101538

Bhuiyan, M. T. R., Hirai, N., and Sobue, N. (2000). "Changes of crystallinity in wood cellulose by heat treatment under dried and moist conditions," *J. Wood Sci.* 46, 431-436. DOI: 10.1007/BF00765800

Bhuiyan, T., and Hirai, N. (2005). "Study of crystalline behavior of heat-treated wood cellulose during treatments in water," *J. Wood Sci.* 51, 42-47. DOI: 10.1007/s10086-003-0615-x

Birinci, E., Karamanoğlu, M., Kesik, H. I., and Kaymakci, A. (2022). "Effect of heat treatment parameters on the physical, mechanical, and crystallinity index properties of Scots pine and beech wood," *BioResources* 17(3), 4713-4729. DOI: 10.15376/biores.17.3.4713-4729

Biziks, V., Andersons, B., Beļkova, Ļ., Kapača E., and Militz, H. (2013). "Changes in the microstructure of birch wood after hydrothermal treatment," *Wood Sci. Technol.* 47, 717-735. DOI: 10.1007/s00226-013-0531-1

Borůvka, V., Dudík, R., Zeidler, A., and Holeček, T. (2019). "Influence of site conditions and quality of birch wood on its properties and utilization after heat treatment. Part I—Elastic and strength properties, relationship to water and dimensional stability," *Forests* 10(2), article 189. DOI: 10.3390/f10020189

Broda, M., Curling, S. F., Spear, M. J., and Hill C. A. S. (2019). "Effect of methyl-trimethoxysilane impregnation on the cell wall porosity and water vapour sorption of archaeological waterlogged oak," *Wood Sci. Technol.* 53, 703-726. DOI: 10.1007/s00226-019-01095-y

Brunauer, S., Emmett, P. H., and Teller, E. (1938). "Adsorption of gases in multimolecular layers," *J. Am. Chem. Soc.* 60(2), 309-319. DOI: 10.1021/ja01269a023

Bryne, L., Lausmaa, J., Ernstsson, M., Englund, F., and Wålinder, M. (2010). "Ageing of modified wood. Part 2: Determination of surface composition of acetylated, furfurylated, and thermally modified wood by XPS and ToF-SIMS," *Holzforschung* 64(3), 305-313. DOI: 10.1515/hf.2010.062

Cai, C. Y., Haapala, A., Rahman, M. H., Tiitta, M., Tiitta, V., Tomppo, L., Lappalainen, R., and Heräjärvi, H. (2020). "Effects of two-year weather exposure on thermally modified *Picea abies*, *Pinus sylvestris*, and *Fraxinus excelsior* wood," *Can. J. Forest Res.* 50, 1160-1171. DOI: 10.1139/cjfr-2019-0446

Cai, C. Y., Javed, M. A., Komulainen, S., Telkki, V.-V., Haapala, A., and Heräjärviet, H. (2020). "Effect of natural weathering on water absorption and pore size distribution in thermally modified wood determined by nuclear magnetic resonance," *Cellulose* 27, 4235-4247. DOI: 10.1007/s10570-020-03093-x

Cai, C. Y., Zhou, F., and Cai, J. (2020). "Bound water content and pore size distribution of thermally modified wood studied by NMR," *Forests* 11(12), article 1279. DOI: 10.3390/f11121279

Cao, S., Cheng, S., and Cai, J. (2022). "Research progress and prospects of wood high-temperature heat treatment technology," *BioResources* 17(2), 3702-3717. DOI: 10.15376/biores.17.2.cao

Cao, Y., Lu, J., Huang, R., Zhao, Y., and Wu, Y. (2011). "Evaluation of decay resistance for steam-heat-treated wood," *BioResources* 6(4), 4696-4704. DOI: 10.15376/biores.6.4.4696-4704

Čermák, P., Vahtikari, K., Rautkari, L., Laine, K., Horáček, P., and Baar, J. (2016). "The effect of wetting cycles on moisture behaviour of thermally modified Scots pine (*Pinus sylvestris* L.) wood," *J. Mater. Sci.* 51, 1504-1511. DOI: 10.1007/s10853-015-9471-5

Cheng, X. Y., Li, X. J., and Xu, K., (2017). "Effect of thermal treatment on functional groups and degree of cellulose crystallinity of eucalyptus wood (*Eucalyptus grandis* × *Eucalyptus urophylla*)," *Forest Prod. J.* 67(1-2), 135-140. DOI: 10.13073/FPJ-D-15-00075

Colom, X., Carrillo, F., Nogués, F., and Garriga, P. (2003). "Structural analysis of photodegraded wood by means of FTIR spectroscopy," *Polym. Degrad. Stabil.* 80(3), 543-549. DOI: 10.1016/s0141-3910(03)00051-x

Czajkowski, Ł., Olek, W., and Weres, J. (2020). "Effects of heat treatment on thermal properties of European beech wood," *Eur. J. Wood Wood Prod.* 78, 425-431 . DOI: 10.1007/s00107-020-01525-w

Durmaz, E., Ucuncu, T., Karamanoglu, M., and Kaymakcı, A. (2019). "Effects of heat treatment on some characteristics of Scots pine (*Pinus sylvestris L.)* wood," *BioResources* 14(4), 9531-9543. DOI: 10.15376/biores.14.4.9531-9543

Dwianto, W., Tanaka, F., Inoue, M. K., and Norimoto, M. (1996). "Crystallinity changes of wood by heat or steam treatment," *Wood Res.* 83, 47-49.

Elisabeth, W., and Gerd, W. (2008). "Behaviour of lignin during thermal treatments of wood," *Ind. Crop. Prod.* 27, 157-162. DOI: 10.1016/j.indcrop.2007.07.015

Endo, K., Obataya, E., Zeniya, N., and Matsuo, M. (2016). "Effects of heating humidity on the physical properties of hydrothermally treated spruce wood," *Wood Sci. Technol.* 50, 1161-1179. DOI: 10.1007/s00226-016-0822-4

Gérardin, P. (2016). "New alternatives for wood preservation based on thermal and chemical modification of wood— A review," *Ann. For. Sci.* 73, 559-570. DOI: 10.1007/s13595-015-0531-4

Guo, J., Song, K., and Salmén, L. (2015). "Changes of wood cell walls in response to hygro-mechanical steam treatment," *Carbohyd. Polym.* 115, 207-214. DOI: 10.1016/j.carbpol.2014.08.040

Hakkou, M., Pètrissans, M., Zoulalian, A., and Gèrardin, P. (2005). "Investigation of wood wettability changes during heat treatment on the basis of chemicals analysis," *Polym. Degrad. Stabil.* 89(1), 1-5. DOI: 10.1016/j.polymdegradstab.2004.10.017

He, L. X., Zhang, T. F., and Zhao, X. Y. (2023). "Synergistic effect of tung oil and heat treatment on surface characteristics and dimensional stability of wood," *Colloid. Surface. A.* 665, article 1233. DOI: 10.1016/j.colsurfa.2023.131233

Hill, C. A. S., Altgen, M., and Rautkari, L. (2021). "Thermal modification of wood—A review: Chemical changes and hygroscopicity," *J. Mater. Sci.* 56, 6581-6614. DOI: 10.1007/s10853-020-05722-z

Hill, C. A. S. (2006). "Wood modification – Chemical, thermal and other processes," Chichester, UK

Hillis, W., and Rozsa, A. (1978). "The softening temperatures of wood," *Holzforschung* 32(2), 68-73. DOI: 10.1515/hfsg.1978.32.2.68

Jang, E. S., and Kang, C. W. (2019). "Changes in gas permeability and pore structure of wood under heat treating temperature conditions," *J. Wood Sci.* 65, article 37. DOI: 10.1186/s10086-019-1815-3

Junghans, K., Niemz, P., and Bächle, F. (2005). "Untersuchungen zum Einfluss der thermischen Vergütung auf die Porosität von Fichtenholz [Investigations into the influence of thermal treatment on the porosity of spruce wood]," *Holz. Roh. Werkst.* 63, 243-244. DOI: 10.1007/s00107-004-0553-3

Kim, U. J., Eom, S. H., and Wada, M. (2010). "Thermal decomposition of native cellulose: infuence on crystallite size," *Polym. Degrad. Stabil.* 95(5), 778-781. DOI: 10.1016/j.polymdegradstab.2010.02.009

Kotilainen, R. A., Toivanen, T. J., and Alén, R. J. (2000). "FTIR monitoring of chemical changes in softwood during heating," *J. Wood Chem. Technol.* 20(3), 307-320. DOI: 10.1080/02773810009349638

Kučerová, V., Lagaňa, R., and Hýrošová, T. (2019). "Changes in chemical and optical properties of silver fir (*Abies alba L.*) wood due to thermal treatment," *J. Wood Sci.* 65, article 21. DOI: 10.1186/s10086-019-1800-x

Kymäläinen, M., Mlouka, S. B., Belt, T., Merk, V., Liljeström, V., Hänninen, T., Uimonen, T., Kostiainen, M., and Rautkari, L. (2018). "Chemical, water vapour sorption and ultrastructural analysis of Scots pine wood thermally modified in high-pressure reactor under saturated steam," *J. Mater. Sci.* 53, 3027-3037. DOI: 10.1007/s10853-017-1714-1

Lê, H. Q., Zaitseva, A., and Pokki, J. P. (2016). "Solubility of organosolv lignin in γ-valerolactone/water binary mixtures," *ChemSusChem* 9(20), 2939-2947. DOI: 10.1002/cssc.201600655

Li, M. Y., Cheng, S. C., Li, D., Wang, S. N., Huang, A. M., and Sun, S. Q. (2015). "Structural characterization of steam-heat treated *Tectona grandis* wood analyzed by FT-IR and 2D-IR correlation spectroscopy," *Chinese Chem. Lett.* 26(2), 221-225. DOI: 10.1016/j.cclet.2014.11.024

Liu, S., Ran, Y. Y., and Cao, J. Z. (2023). "Comparison on thermally modified beech wood in different mediums: Morphology, chemical change and water-related properties," *Ind. Crops Prod.* 209, article ID 117935. DOI: 10.1016/j.indcrop.2023.117935

Marcon, B., Tondi, G., Procino, L., and Goli, G. (2021). "Thermal modification kinetics and chemistry of poplar wood in dry and saturated steam media," *Holzforschung* 75(8), 721-730. DOI: 10.1515/hf-2020-0166

Newman, R. H. (1999). "Estimation of the lateral dimensions of cellulose crystallites using 13C NMR signal strengths solid state," *Solid State Nucl. Mag.* 15(1), 21-29. DOI: 10.1016/s0926-2040(99)00043-0.

Nuopponen, M. (2005). *FT-IR and UV-Raman Spectroscopic Studies on Thermal Modification of Scots Pine Wood and Its Extractable Compounds*, Doctor's Thesis, Helsinki University of Technology, Espoo, Finland. DOI: 10.1360/biodiv.050121

Obataya, E., and Tomita, B. (2002). "Hygroscopicity of heat-treated wood. II Reversible and irreversible reductions in the hygroscopicity of wood due to heating," *Mokuzai Gakkaishi (Journal of the Japan Wood Society)* 48(4), 288-295.

Obataya, E., and Higashihara, T. (2017). "Reversible and irreversible dimensional changes of heat-treated wood during alternate wetting and drying," *Wood Sci. Technol.* 51, 739-749. DOI: 10.1007/s00226-017-0918-5

Obataya, E., Zeniya, N., and Endo, K. (2021). "Effects of water-soluble extractives on the moisture sorption properties of spruce wood hygrothermally treated at 120 °C and different humidity levels," *Wood Mater. Sci. Eng.* 16(2), 124-131. DOI: 10.1080/17480272.2019.1635642

Olek, W., and Bonarski, J. T. (2014). "Effects of thermal modification on wood ultrastructure analyzed with crystallographic texture," *Holzforschung* 68(6), 721-726. DOI: 10.1515/hf-2013-0165

Özgenç, Ö., Durmaz, S., Boyaci, I. H., and Haslet, E. K. (2017). "Determination of chemical changes in heat-treated wood using ATR-FTIR and FT Raman spectrometry," *Spectrochim. Acta. A* 171, 395-400. DOI: 10.1016/j.saa.2016.08.026

Pelit, H., Budakçı, M., and Sönmez, A. (2016). "Effects of heat post-treatment on dimensional stability and water absorption behaviours of mechanically densified Uludağ fir and black poplar woods," *BioResources* 11(2), 3215-3229.

Peng, Q., Ormondroyd, G., Spear, M., and Chang, W. S. (2022). "The effect of the changes in chemical composition due to thermal treatment on the mechanical properties of *Pinus densiflora*," *Constr. Build. Mater.* 358, article 129303. DOI: 10.1016/j.conbuildmat.2022.129303

Phuong, L., Takayama, M., Shida, S., Matsumoto, Y., and Aoyagi, T. (2007). "Determination of the accessible hydroxyl groups in heat-treated *Styrax tonkinensis* (Pierre) Craib ex Hartwich wood by hydrogen-deuterium exchange and 2H NMR spectroscopy," *Holzforschung* 61(5), 488-491. DOI: 10.1515/HF.2007.086

Pockrandt, M., Jebrane, M., Cuccui, I., Allegretti, O., Uetimane, E., and Terziev, N. (2018). "Industrial Thermowood® and Termovuoto thermal modification of two hardwoods from Mozambique," *Holzforschung* 72(8), 701-709. DOI: 10.1515/hf-2017-0153

Rahimi, S., Singh, K., and DeVallance, D. (2019). "Effect of different hydrothermal treatments (steam and hot compressed water) on physical properties and drying behavior of yellow-poplar (*Liriodendron tulipifera*)," *Forest Prod. J.* 69(1), 42-52. DOI: 10.13073/FPJ-D-18-00028

Shi, J., and Avramidis, S. (2018). "Dried cell wall nanopore configuration of Douglas-fir, western red cedar and aspen heartwoods," *Wood Sci. Technol.* 52, 1025-1037. DOI: 10.1007/s00226-018-1011-4

Sikora, A., Kačík, F., Gaff, M., Vondrová, V., Bubeníková, T., and Kubovský, I., (2018). "Impact of thermal modification on color and chemical changes of spruce and oak wood," *J. Wood Sci.* 64, 406-416. DOI: 10.1007/s10086-018-1721-0

Sun, B., Su, Y., Wang, X., and Chai, Y. (2022). "The influence of vacuum heat treatment on the pore structure of earlywood and latewood of larch," *Holzforschung* 76(11-12), 985-993. DOI: 10.1515/hf-2022-0107

Temiz, A., Terziev, N., Eikenes, M., and Hafren, J. (2007). "Effect of accelerated weathering on surface chemistry of modified wood," *Appl. Surf. Sci.* 253(12), 5355-5362. DOI: 10.1016/j.apsusc.2006.12.005

Thygesen, A., Oddershede, J., Lilholt, H., Thomsen, A. B., and Ståhl, K. (2005). "On the determination of crystallinity and cellulose content in plant fibres," *Cellulose* 12, 563-576. DOI: 10.1007/s10570-005-9001-8

Wang, D., Fu, F., and Lin, L. (2022). "Molecular-level characterization of changes in the mechanical properties of wood in response to thermal treatment," *Cellulose* 29, 3131-3142. DOI: 10.1007/s10570-022-04471-3

Wang, P., and Howard, B. H. (2018). "Impact of thermal pretreatment temperatures on woody biomass chemical composition, physical properties and microstructure," *Energies* 11(1), article 25. DOI: 10.3390/en11010025

Wang, X., Chen, X., Xie, X., Wu, Y., Zhao, L., Li, Y., and Wang, S. (2018). "Effects of thermal modification on the physical, chemical and micromechanical properties of Masson pine wood (*Pinus massoniana Lamb.*)," *Holzforschung* 72(12), 1063-1070. DOI: 10.1515/hf-2017-0205

Willems, W., Altgen, M., and Rautkari, L. (2020). "A molecular model for reversible and irreversible hygroscopicity changes by thermal wood modification," *Holzforschung* 74(4), 420-425. DOI: 10.1515/hf-2019-0057

Windeisen, E., Strobel, C., and Wegener, G. (2007). "Chemical changes during the production of thermo-treated beech wood," *Wood Sci. Technol.* 41, 523-536. DOI: 10.1007/s00226-007-0146-5

Wu, Z., Deng, X., Li, L., Xi, X., Tian, M., Yu, L., and Zhang, B. (2021). "Effects of heat treatment on interfacial properties of *Pinus massoniana* wood," *Coatings* 11(5), article 543. DOI: 10.3390/coatings11050543

Xu, J. W., Li, C. C., and Hung, K. C. (2022). "Physicomechanical properties of hydrothermally treated Japanese cedar timber and their relationships with chemical compositions," *J. Mater. Res. Technol.* 21, 4982-4993. DOI: 10.1016/j.jmrt.2022.11.092

Yin, J., Song, K., Lu, Y., Zhao, G. J., and Yin, Y. F. (2015). "Comparison of changes in micropores and mesopores in the wood cell walls of sapwood and heartwood," *Wood Sci. Technol.* 49, 987-1001. DOI: 10.1007/s00226-015-0741-9

Zauer, M., Pfriem, A., and Wagenführ, A. (2013). "Toward improved understanding of the cell-wall density and porosity of wood determined by gas pycnometry," *Wood Sci. Technol.* 47, 1197-1211. DOI: 10.1007/s00226-013-0568-1

Zhao, X., Wang, T., He, L., Zhang, T., Gao, J., He, Z., and Yi, S. (2023). "Hygroscopicity and dimensional stability of wood thermally treated with moist air or low point metal alloy: A comparative study," *Holzforschung* 77(1), 28-37. DOI: 10.1515/hf-2022-0101

Zheng, A. Q., Jiang, L. Q., Zhao, Z. L., Chang S., Huang, Z., Zhao, K., He, F., and Li, H. B. (2016). "Effect of hydrothermal treatment on chemical structure and pyrolysis behavior of eucalyptus wood," *Energ. Fuel* 30(4), 3057-3065. DOI: 10.1021/acs.energyfuels.5b03005

Zyłka, R., Kleszczyńska, H., Kupiec, J., Bonarska-Kujawa, D., Hladyszowski, J., and Przestalski, S. (2009). "Modifications of erythrocyte membrane hydration induced by organic tin compounds," *Cell Biol. Int.* 33(7), 801-806. DOI: 10.1016/j.cellbi.2009.04.016

Article submitted: July 4, 2024; Peer review completed: August 2, 2024; Revised version received and accepted: August 5, 2024; Published: August 21, 2024.
DOI: 10.15376/biores.19.4.7320-7338